PHYSICAL REVIEW E, VOLUME 64, 021506

Molecular dynamics study of the stability of the hard sphere glass

S. R. Williams, I. K. Snook, and W. van Megen
Department of Applied Physics, Royal Melbourne Institute of Technology, Melbourne, Victoria 3001, Australia

(Received 9 January 2001; published 19 July 2001)

Glassy states have been observed in hard-spherelike colloidal suspensions; however, some recent work suggests that a stable, one-component hard-sphere glass doesn't exist. A possible resolution of this dilemma is that colloidal glass formation results from a small degree of particle polydispersity. In order to investigate this further, we used the molecular-dynamics method to explore the phase behavior of both one- and two-component hard-sphere systems. It was found that the metastable fluid branch of the one-component system ceased to exist at a volume fraction marginally above melting, instead this system always crystallized within a relatively short period of time. Binary systems with a size ratio $\gamma = 0.9$ were then used as the simplest approximation to model a polydisperse hard-sphere colloidal system. Here the crystallization process was slowed down dramatically for all volume fractions and the fluid state was maintained for many relaxation times. Indeed, at the lowest volume fraction $\phi = 0.55$ no sign of crystallization was seen on the simulation time scale. The systems at intermediate volume fractions did eventually crystallize but at the highest volume fraction of $\phi = 0.58$, a dramatic slowing down in the crystallization process was observed. This is qualitatively in agreement with the experimental results on colloidal suspensions. Using the insight gained from this paper, the reasons behind a polydisperse system forming a stable glass, in contrast to the one-component system, are elucidated.

DOI: 10.1103/PhysRevE.64.021506 PACS number(s): 64.70.Pf

I. INTRODUCTION

One of the most interesting results from the pioneering computer simulation studies of Alder and Wainwright [1] and of Wood and Parker [2] was that a system of purely repulsive hard spheres in periodic boundary conditions can exist in both a fluidlike state and a crystalline state (these states being linked by first-order phase transition). Subsequent simulation studies indicated that the hard-sphere system may also form a long-lived glassy state. In order to explore the question of hard-sphere glass formation, Woodcock [3] introduced schemes for compressing the equilibrium hard-sphere fluid to a supercooled fluid state. His results seemed to indicate the existence of a glassy state for the one-component hard-sphere system. More recently Pusey and van Megen [4] determined that a hard-spherelike colloidal suspension not only exhibited an equilibrium fluid and solid phase, but at high densities a long-lived glassy phase was also observed after shear melting. Despite the small amount of polydispersity, (defined as the standard deviation of the particle size distribution divided by the mean size, s) of around $s = 0.05$, the observed equilibrium phase behavior could be accurately mapped to that predicted for a one-component hard-sphere system by computer simulation [5]. This observation is consistent with more recent computational work [6] where only subtle changes in the experimentally observable properties (Pusey and van Megen) are predicted for the equilibrium phase behavior of a system with this amount of polydispersity, compared to a monodisperse system.

Despite the results of this early work there is increasing evidence from computer-simulation studies that monodisperse hard-sphere systems do not form a stable glassy phase [7,8]. However the mechanisms responsible for this difference in behavior between monodisperse and polydisperse hard-sphere systems are yet to be elucidated.

Here we have made a theoretical study of hard-sphere systems using the molecular-dynamics (MD) method to provide some insight into the occurrence and suppression of crystallization. Simulations of one-component systems are used to confirm that deeply quenched fluids are indeed unstable and crystallize rapidly. We have studied this over a larger range of volume fractions and for a longer duration of time than has been done in previous work.

Although simulating the crystallization of a one-component hard-sphere system is now a relatively easy task, extending such studies to a model of a truly polydisperse system is quite difficult due to the added complexity in calculating the precise and relevant phase behavior. Hence we have carried out hard-sphere MD simulations using a binary system with a size ratio $\gamma = 0.905$ to investigate the problem as a first step towards modeling a truly polydisperse system with a small value of s. While it might be thought that such a binary system is somewhat different from a typical colloidal dispersion of narrow size distribution, we found that the crystallization process is significantly retarded, relative to the one-component system, and that behavior is seen which mimics that observed in such colloidal systems. More importantly the reasons for the crystallization processes being suppressed in the binary system are shown here to be both readily understandable and to be relevant to understanding the behavior of the polydisperse system.

II. SIMULATION DETAILS

Molecular-dynamics simulations of one- and two-component hard-sphere systems were performed in periodic boundary conditions in which the total number of particles N, the system's volume V, and the internal energy U were held fixed, i.e., we used a microcanonical ensemble. The

1063-651X/2001/64(2)/021506(7)/$20.00

hard-sphere system has no potential energy; thus if the internal energy is held fixed, the temperature T will also be held fixed, and the microcanonical ensemble is equivalent to the canonical ensemble. The computational procedures are standard and extensively documented [9]. All length scales in the simulations are expressed in terms of σ_1, the diameter of the particles of species one, and the binary systems have a size ratio $\gamma = \sigma_1/\sigma_2 = 0.905$. Rather than the number density ρ, the volume fraction ϕ will be used to define particle concentration, which is defined as the total volume of all the particles in the simulation divided by the volume of the simulation box. For the one-component system we have

$$\phi = \frac{\pi N \sigma^3}{6V} = \frac{\pi\sigma^3}{6}\rho \tag{1}$$

and for the binary system we have

$$\phi = \frac{\pi(N_1\sigma_1^3 + N_2\sigma_2^3)}{6V} = \frac{\pi\sigma_1^3}{6}\rho\left(\frac{N_1}{N} + \frac{N_2}{N}\frac{1}{\gamma^3}\right). \tag{2}$$

To a first approximation this allows one to directly compare the binary system to a corresponding one-component system as, in contrast to the number density, the volume fraction allows the construction of a phase diagram that is invariant to the particle diameter σ. The volume fractions of freezing and melting for one-component hard spheres are 0.494 and 0.545, respectively [5]. The binary systems used were such that both species had the same mass, $m_1 = m_2 = m$, and were equimolar, $N_1 = N_2 = N/2$. All times were measured in units of $\sigma_1\sqrt{m/kT}$, as such a particle of species one undergoing ballistic dynamics will, on root-mean-square average, travel its own diameter in a dimensionless time of $1/\sqrt{3}$. The polydispersity of equimolar binary systems with $\gamma < 1$ is given by

$$s = 1 - \frac{2\gamma}{1+\gamma}, \tag{3}$$

which for the present system gives $s = 0.05$. The one-component system used had a system size $N = 864$, which was found to be large enough to allow rapid crystallization, which was all that was of interest concerning a one-component system for this paper. The binary system size chosen had $N = 10\,976$, the larger system size was necessary for the more detailed study performed to find out what microscopic mechanisms are retarding the crystallization process.

The pressure p or compressibility factor $Z = pV/NkT$ and system radial distribution function $g(r)$ were monitored to give a gross indication of the stability of the system. In fact, as the pressure difference between the quenched fluid and the crystal is quite pronounced in the NVT system, the observation of a falling pressure was interpreted as being an indicative measure of crystallization. While this is a rather unsophisticated approach it was only used as an overall indication as to the physical phase present.

In order to follow the process of crystallization we need a more detailed picture of the local microscopic structure or environment of each atom in the system. In general it is difficult to unambiguously classify and analyze the structure of systems having only local order, such as nucleating fluids. Voronoi analysis has been extensively used to study amorphous materials, crystalline materials [10,11], and to follow the process of crystallization [12–15]. The Voronoi method decomposes space into a set of polyhedra associated with each particle. The polyhedron for each particle is defined as the region of space closer to that particle than it is to any other particle in the material. Often the shape of these Voronoi cells are used directly to measure the local environment of each particle and to infer something about the degree of crystalline order present. However there are some problems involving degeneracies of the faces of these polyhedra [16]. In fact distortions of the shape of the Voronoi polynedra by such effects as thermal motion makes it difficult to measure the fcc and hcp local environments in nucleating systems. Thus in the traditional Voronoi method [10,11] fcc and hcp environments are unstable with respect to thermal distortions. Methods have been suggested to improve this analysis, which are not entirely without problems. Thus we have developed a new method to identify the local fcc or hcp environments in a nucleating system [16].

Another method used to analyze systems, which are lacking in long-range order, is ring statistics. Here a measure of the connectivity of the atoms in the system is sought. Many definitions of these rings are possible, however Franzblau [17] showed that it is possible to define a set of rings by a shortest-path criterion, which is probably the most natural and consistent way of performing a ring analysis. The resultant measure of local structure is shown to agree well with intuitive ideas about short-to medium-range structure, and in a hierarchy of criteria for constructing such rings it falls exactly midway between the least restrictive and most restrictive criteria possible. Thus, we have combined the Voronoi and ring statistics methods in order to provide a reasonable measure of the local structure around each particle. This process involves two steps. First the bond network is determined using a modified Voronoi decomposition. Second the local structure of a given particle is determined. This involves taking all the particles bonded to the chosen particle and determining their topology from the bonds between them, excluding the chosen particle, using the shortest-path ring criterion. This prescription was carried directly over to the binary systems studied here. We found that the method was readily and unambiguously able to find those particles that have a fcc and those that have a hcp local environment. This proved to be sufficient to characterize the crystallization process at the microscopic level.

In order to prepare the quenched states, a low-density equilibrium fluid configuration was increased in density by an amount $d\rho$ every dt time intervals by scaling the particle positions. The configuration is then corrected for any spheres that slightly overlap by simply moving them apart the minimum necessary distance. This process is repeated until no spheres are overlapping with the simulation and then are allowed to run for another time interval of dt. The change in density $d\rho$ is small and the process approximates a constant quench rate $d\rho/dt$. We have found our results to have little sensitivity on the quench rate within reasonable limits. The effect of quench rate will not be investigated further in this paper. The values used for the change in density and the time interval in the presented paper are $d\rho = 0.025$ and $dt = 0.04$. All quenches were started from an equilibrated fluid at a volume fraction of $\phi = 0.3$.

We find it necessary to identify a relaxation time for the fluids studied. In general the relaxation time will depend on the dynamical quantity under consideration, however, as much experimental work has been done measuring and characterizing intermediate scattering functions around the peak of the static structure factor in colloidal systems, we allow this to influence our relaxation-time scale. Drawing upon the work of van Megen *et al.* [18] we define the following estimate of the fluid relaxation time τ as a reasonable one for the purposes at hand

$$\langle \Delta r(\tau)^2 \rangle \approx 0.25. \tag{4}$$

This is the time a particle takes to diffuse a distance equal to its own radius in the length units used here. The mean-square displacement was calculated directly from the particle trajectories, and in the case of the binary fluid, the small and the large spheres were not discriminated between. The long-time linear regime of the mean-square displacement was used to calculate the long-time diffusion coefficient.

III. RESULTS AND DISCUSSION

A. Phase behavior

In this section the detailed phase behavior of an equimolar hard-sphere system having a size ratio of $\gamma = 0.9$, is presented along with the way it was determined. As it turns out the approach of presenting the phase behavior, at a fixed total composition, as a function of the total volume fraction, provides important insight to the problem at hand. These are the conditions, after all, under which an experimental colloidal system is constrained, that is upon changing the volume fraction of such a system, its particle-size distribution remains unaltered [4,19,20]. Other work on the phase behavior of binary and polydisperse hard-sphere systems, either fails to acknowledge this important aspect, or does not examine it in the detail presented here. Some of the results in this section will be drawn upon later.

The detailed phase behavior of the binary system is more complicated, than the one-component system, due to its extra thermodynamic degree of freedom. This results in the composition of both the liquid and the solid phases changing, as a function of the total volume fraction, as the coexistent liquid-solid and solid-solid regions are traversed. In contrast to the one-component system, this results in the pressure of the binary system varying as the coexistent liquid-solid region is traversed.

Along with several other size ratios the phase diagrams of binary hard spheres with size ratio $\gamma = 0.9$, have been calculated by Kranendonk and Frenkel [21]. In addition to the coexistent fluid-crystal region this system has a coexistent crystal-crystal region at high volume fractions. Their work shows which compositions coexist at a given pressure for both fluid-crystal and crystal-crystal regions. It also presents the melting and freezing volume fractions as a function of composition. The data from this paper has been manipulated in order to obtain the desired phase diagram for our current purposes. In addition, any fluid equation of state data necessary was obtained from the expression of Mansoori *et al.* [22] and any crystal equation of state data was obtained from molecular dynamics (MD) simulations of fcc crystals. We have verified by MD calculations that, below melting, the expression of Mansoori *et al.* [21] gives results to an accuracy of better than 1% for the equation of state data under consideration.

In order to proceed we write down the equations which constrain the system in the desired fashion. First we define the variable p as follows,

$$p = \frac{V_f}{V_T}, \quad 1 - p = \frac{V_s}{V_T}, \tag{5}$$

where V_f is the volume of the fluid phase, V_s is the volume of the solid phase, and V_T is the total volume of the system. We already know the volume fractions of the coexisting fluid ϕ_f and solid ϕ_s phases [21], but we need to find the correct value for p, which gives the required total composition of $X_T = 0.5$. The total volume fraction ϕ_T of the system may now be expressed in terms of the variables so far defined

$$\phi_T = p\,\phi_f + (1-p)\,\phi_s\,. \tag{6}$$

The total composition of the system may also be expressed in terms of the composition of the fluid X_f and solid X_s phases

$$X_T = X_s \frac{\rho_s}{\rho_T}(1-p) + X_f \frac{\rho_f}{\rho_T} p = 0.5, \tag{7}$$

where ρ_s, ρ_f, and ρ_T are the number densities of the solid and fluid phases and of the total system, respectively. Let the number density be represented by ρ_x, the volume fraction by ϕ_x and the composition by X_x, where x may be defined as equivalent to s,f or T as required, then the three equations relating the number density to the volume fraction are

$$\rho_x = \frac{6\phi_x}{\pi} \frac{1}{(1 - X_x + X_x/\gamma^3)}. \tag{8}$$

The five equations [Eqs. (6), (7), and (8)] thus allow the determination of the five unknowns ϕ_T, p, and ρ_x. These equations were solved using iterative techniques. The coexistent crystal crystal region was determined in the exact same manner; in this case the subscript f denoted the second solid phase.

The dimensionless pressure given by $P^* = Z\phi$, where Z is the compressibility factor as a function of volume fraction, may be seen in Fig. 1 for the fluid and crystal phases of both the one-component and binary systems. This gives a pressure unit that would be, in general, dependent on the composition, however, as we are keeping the total composition fixed and investigating the pressure of the total system, this is of no consequence. However, as this dimensionless pressure is invariant to changes in the fundamental length scale of the

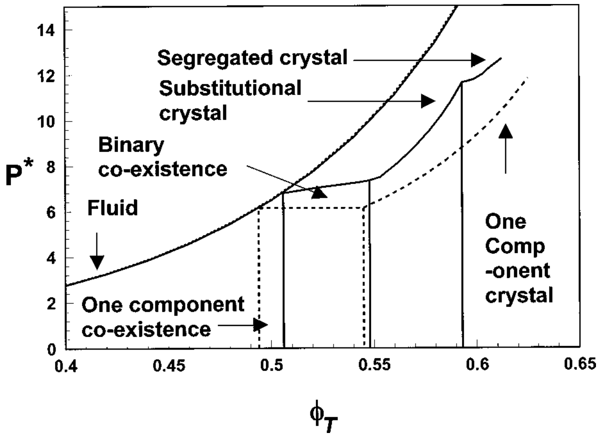

FIG. 1. A comparison of the phase diagrams of the one-component hard-sphere system (dashed lines) and an equimolar, two-component hard-sphere system with a radius ratio of 0.9 (solid lines).

system, it allows a direct comparison between the binary and one-component systems. It can be seen that the equilibrium fluid pressure is perturbed very little in going from the one-component to the binary system. The coexistent regions for both systems can be readily seen, with the binary system having a freezing point above that of the one-component system. Unlike the one-component system the pressure of the binary system increases in going from freezing to melting. To understand this, recall that for the binary system, in contrast to the one-component system, the two coexisting phases will have individual volume fractions and compositions that change as the coexistent region is traversed. Above melting, the binary system has a substitutional crystal branch that has a significantly higher pressure than the corresponding one-component crystal. At the volume fraction of $\phi = 0.593$ the binary system undergoes a phase change from a single substitutional crystal to two coexisting substitutional crystals of different compositions [21]. At close packing $\phi = 0.740$, two coexistent one-component crystals would be obtained, one for each species [23]. The composition and amount of crystal as a function of volume fraction for the various phases of the binary system, are shown in Figs. 2(a) and 2(b), respectively. It can be readily seen that just above freezing, the solid phase is richer in large particles than the total system. Crystallization from the melt will thus involve compositional rearrangements between the two phases in this region. On the other hand, crystallization from the melt just below melting will involve very little compositional rearrangement. Here we would start with a fluid having the composition of the total system and finish with an equilibrium state of nearly all crystal having a composition very close to the total composition of the system. Also of interest is that the amount of crystal in going from freezing to melting is not a linear function of volume fraction as it is for the one-component system, see Fig. 2(b). As has already been mentioned, the implications that the work discussed in this section has on the stability of the quenched fluid branch, will be discussed in more detail later.

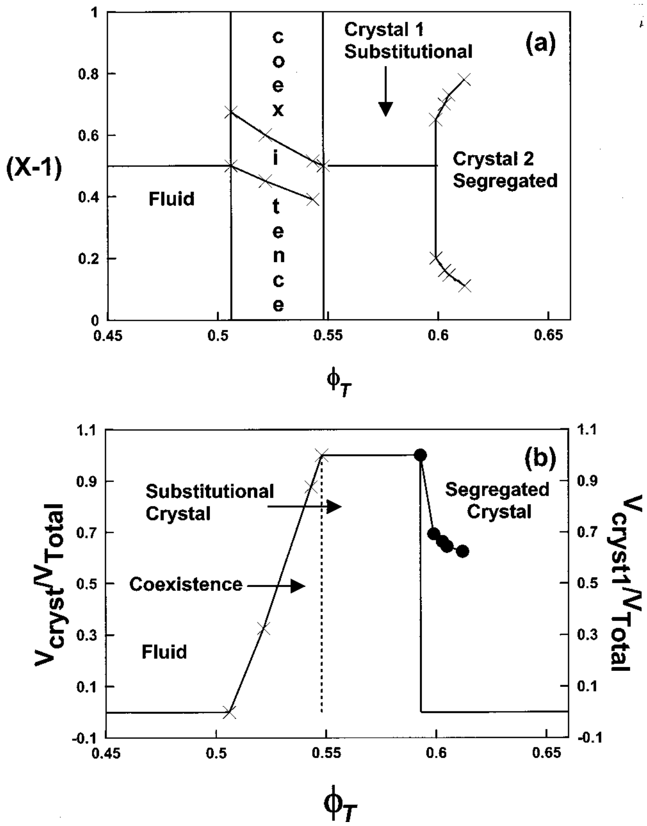

FIG. 2. (a) The composition X of the equilibrium phases as a function of the systems total volume fraction ϕ_T for the two-component system. Shown are the regions of stability of the fluid, coexisting fluid solid, substitutional crystal (crystal 1) and the segregated crystal (crystal 2). (b) The total volume of crystal in the system relative to the total volume, $V_{\mathrm{cryst}}/V_{\mathrm{Total}}$ shown as crosses and the total volume of crystal 1 in the system relative to the total volume, $V_{\mathrm{crystal}}/V_{\mathrm{Total}}$ shown as filled circles versus the total volume fraction of the system ϕ_T.

IV. CRYSTALLIZATION RATES

Here the crystallization process as a function of volume fraction was investigated for both the one-component and binary systems. In order to see if the metastable states produced in these studies are truly long lived or not, we first had to obtain a realistic measure of the relaxation time in the stable fluid. This was so that we can quantify the meaning of long lived in this context. Now, experimentally small changes in polydispersity have been found to have a much more critical effect on crystallization rates than on fluid dynamics for polydispersities around $s = 0.06$ [20]. As the binary fluids turn out to be considerably more stable than their one-component counterparts, the relaxation times found for the binary fluids will be assumed to be valid for both. The relaxation times at various volume fractions ϕ may be seen in Table I along with the long-time diffusion coefficients and the time taken by the systems to undergo significant crystallization.

The compressibility factor Z of the one-component system as a function of time for several volume fractions at and above melting, may be seen in Fig. 3. As can be seen, the

TABLE I. Diffusion constants and characteristic times for the hard-sphere systems studied.

Volume fractions, ϕ	Relaxation time[a]	Diffusion coefficient[b]	Crystallization times, one-component system	Crystallization times, binary system
0.55	11.36	0.022	75	>4000
0.56	25.0	0.010	75	2250
0.57	83.3	0.003	50	1600
0.58	500	0.0005	50	>4000

[a] Estimated using Eq. (4).

[b] Measured from the long-time behavior of the mean-square displacement.

crystallization process was very fast. Immediately after the quench, the pressure fell rapidly to a value close to the pressure of the metastable fluid branch for the polydisperse system. Shortly after this the pressure fell again, this time due to the system crystallizing. This information is used to obtain a rough estimate of the time scale on which the system undergoes significant crystallization, see Table I. Still referring to Table I, we compare the crystallization times to the fluid's relaxation times. At the lowest volume fraction of $\phi = 0.545$, the fluid's relaxation time was found to be some five times less than the crystallization time, however, as the volume fraction was increased, it was found that the relaxation time increased dramatically while the crystallization time underwent very little change, until at the highest volume fraction of $\phi = 0.58$, it was found that the relaxation time was some ten times greater than the crystallization time. Clearly the metastable fluid branch ceases to exist at a volume fraction significantly lower than the experimental glass transition volume fraction of $\phi_g = 0.575$ [18]. This is in agreement with other recent studies using computer-simulation techniques [7,8]. Older studies indicating such a metastable fluid state clearly used too few particles and/or were not of sufficient duration to observe crystallization [3,24]. Importantly our results showed little dependence on quench history.

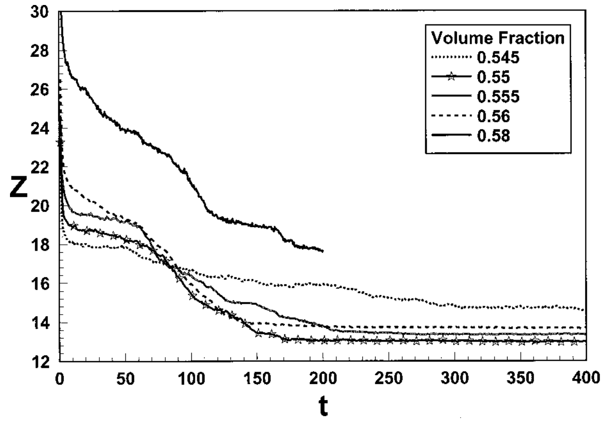

FIG. 3. The compressibility factor $Z = pV/NkT$ as a function of time in reduced units for various volume fractions for the one-component hard-sphere system.

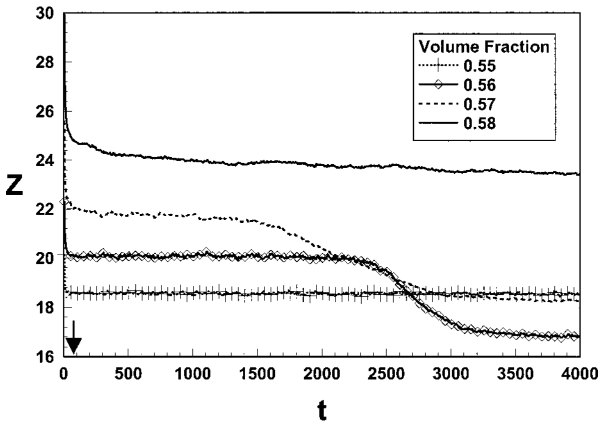

FIG. 4. The compressibility factor $Z = pV/NkT$ as a function of time in reduced units for various volume fractions for the two-component hard-sphere system. The arrow on the time axis indicates the approximate time it takes for the one-component system to crystallize.

This is very different to experimental results on colloidal systems, where long-lived metastable states are observed, allowing measurements on stationary states to be obtained. In fact colloidal systems have been found to undergo a maximum nucleation rate somewhere near melting with the crystallization process slowing down dramatically, at higher volume fractions, as the glass transition is approached [19]. In contrast the one-component system here crystallizes rapidly at these high volume fractions. It should be noted that the small system size of the one-component simulations could retard the crystallization process, thus using a larger system can only decrease the lifetime of these unstable fluid states further. As we have no other interest here in the one-component system other than to illustrate how unstable the dense fluid states above melting are, larger simulations were not carried out in this paper.

The equivalent data for the binary system are shown in Fig. 4. Here we see that the crystallization process was slowed down dramatically for all volume fractions by a minimum of a factor of 30. Importantly the fluid state was maintained for many relaxation times at all volume fractions before significant crystallization took place, as may be seen in Table I. Thus, in this case, the dynamics of the fluid state calculated over this time can be taken to measure the behavior of a true stationary state. While the lowest volume fraction $\phi = 0.55$ showed no sign of crystallization on the simulation time scale, the systems at intermediate volume fractions did show very slow crystallization. However, at the highest volume fraction of $\phi = 0.58$, a dramatic slowing down in the crystallization process was once again observed. The above behavior is qualitatively in agreement with the experimental colloid results discussed above and, thus, we will now explore the underlying reasons for this behavior.

It is normally assumed that the rate of crystallization is controlled by a combination of thermodynamic driving force and diffusional mobility [25]. Thus, in order to start to gain a deeper understanding of the above results, we will refer back to the phase diagrams in Fig. 1 of both the one-component and binary systems. It can readily be seen that the pressure of

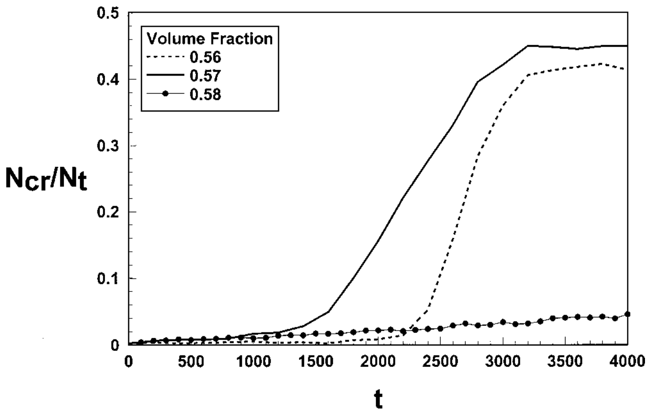

FIG. 5. The number of hard spheres having an fcc or hcp local environment, N_{cr} relative to the total number N_t as a function of time for the two-component hard-sphere system.

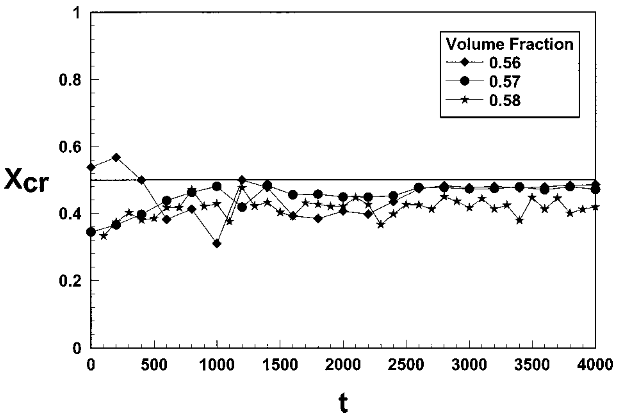

FIG. 6. The composition X_{cr} of hard spheres having a local crystalline environment as a function of time for the two-component hard-sphere system.

the substitutional crystal is significantly higher than that of the corresponding one-component crystal. This isn't surprising as the substitutional crystal packs with less efficiency than the one-component crystal. In contrast to this there is little difference between the pressures of the binary and one-component fluids. This results in a lower thermodynamic driving force, at volume fractions above melting, for the binary system and in turn much longer crystallization times. Figure 4 shows that the binary system at the volume fraction of $\phi = 0.55$, does not crystallize on the experimental MD time scale due to the lack of thermodynamic drive. However, as the volume fraction is increased, the substitutional crystal becomes more and more thermodynamically favored over the fluid. This results in the crystallization process starting at shorter and shorter times. However at the volume fraction of $\phi = 0.58$, the crystallization process has once again become suppressed, even though at this volume fraction there is a large thermodynamic drive for the crystallization process. As we shall see in the next section, this is due to the compositional differences required for the crystallization process to proceed at such a high volume fraction, which can only arise from large scale diffusional processes, which have become greatly suppressed.

V. RING STATISTICS AND STRUCTURAL CHANGES DURING CRYSTALLIZATION

In the previous section we discussed the thermodynamic considerations behind the observed behavior of the metastable state in a binary hard-sphere fluid of small polydispersity. Here we wish to discuss some of the underlying microscopic structural causes of this behavior.

As discussed in Sec. II we use ring statistics to characterize the local atomic structure of the system and, in particular, obtain both the number and type of particles with local fcc and hcp environments as a function of time. The number of particles N_x thus labeled as hcp or fcc, as a function of time for the binary system, are shown in Fig. 5. By comparing this data to Fig. 4, one sees that the pressure is indeed a good indicator of the degree of crystallinity. The composition of the crystal X_{cr} as a function of time is shown in Fig. 6. It can be seen that the crystal is slightly richer in large spheres. It is not hard to envisage that the placement of the small spheres in the substitutional crystal reduces packing efficiency. While the composition of the crystal may not seem very different to that of the total system, the difference is certainly of statistical significance. To demonstrate this imagine we have an infinitely large supply of two types of particles, species 1 and 2. When we select one of these particles at random, the probability of its identity being species 1 is given by the total composition of the system $X_T = 0.5$. Let us randomly select N_x particles from the supply and thus obtain some random composition N_r. We then calculate the probability of this random composition X_r being less than the composition obtained for X_{cr} in the simulation. The results from this binomial distribution problem [26] show the probability to be less than 1% from the time any significant amount of crystal has formed. This demonstrates that the crystallization process requires systematic compositional changes in going from the fluid to the equilibrium substitutional crystal. It should be noted that this is still below the volume fraction of $\phi = 0.593$, above which the equilibrium state consists of two substitutional crystal phases. The required compositional changes demand large-scale diffusion, however, it is large-scale diffusion that is suppressed upon approaching the glass transition, as can be seen from the behavior of the diffusion coefficient shown in Table I. Thus the binary system forms a stable glass while the arrest of large-scale diffusion does little to inhibit crystallization in the case of the one-component system. In this case only local rearrangements are needed to produce a crystalline arrangement from a dense fluid arrangement.

VI. CONCLUSIONS

The one-component hard-sphere fluid has been found to be unstable above the melting volume fraction. It is not stable for times long relative to measured relaxation times and it is not meaningful to talk of a metastable fluid for such a system. It may be that metastable states can be stabilized by using very small systems [3,24]. However, an equimolar binary hard-sphere system with size ratio $\gamma = 0.905$, has been found to have a long-lived, metastable fluid branch above melting. Two separate mechanisms resulting in this difference have been established. At volume fractions slightly above melting, the binary system has a reduced thermodynamic drive due to the reduced packing efficiency of the substitutional crystal. At higher volume fractions the thermodynamic drive rises, which favors crystallization, however here the crystallization process is found to necessitate compositional changes even at volume fractions where the equilibrium phase is a single substitutional crystal. These compositional changes demand large-scale diffusion, which is a property that slows down dramatically with increasing volume fraction; once again crystallization becomes inhibited leading to a long-lived metastable disordered system. Thus, we conclude that a stable glassy phase exists for binary systems, which is not the case for the one-component system.

[1] B. J. Alder and T. E. Wainwright, J. Chem. Phys. **33**, 1439 (1960).

[2] W. W. Wood and J. D. Jacobson, J. Chem. Phys. **27**, 1207 (1957).

[3] L. V. Woodcock, Ann. N.Y. Acad. Sci. **37**, 274 (1981), and references therein.

[4] P. N. Pusey and W. van Megen, Nature (London) **320**, 340 (1986).

[5] W. G. Hoover and F. H. Ree, J. Chem. Phys. **49**, 3609 (1968).

[6] P. G. Bolhuis and D. A. Kofke, Phys. Rev. E **54**, 634 (1996).

[7] I. Moriguchi, K. Kawasaki, and T. Kawakatsu, J. Phys. II **5**, 143 (1995).

[8] M. D. Rintoul and S. Torquato, Phys. Rev. Lett. **77**, 4198 (1996); J. Chem. Phys. **105**, 9258 (1996).

[9] D. C. Rapaport, *The Art of Molecular Dynamics Simulation* (Cambridge University, Cambridge, 1995); M. P. Allen and D. J. Tildesley, *Computer Simulation of Liquids* (Clarendon, Oxford, 1987).

[10] J. D. Bernal and J. L. Finney, Discuss. Faraday Soc. **43**, 60 (1967).

[11] J. L. Finney, Proc. R. Soc. London, Ser. A **319**, 479 (1970).

[12] M. Tanemura, Y. Hiwatari, H. Matsuda, T. Ogawa, N. Ogita, and A. Ueda, Prog. Theor. Phys. **58**, 1079 (1977); **59**, 323 (1978).

[13] C. S. Hsu and A. Rahman, J. Chem. Phys. **71**, 4974 (1979).

[14] J. N. Cape, J. L. Finney, and L. V. Woodcock, J. Chem. Phys. **75**, 2366 (1981).

[15] W. C. Swope and H. C. Anderson, Phys. Rev. B **41**, 7042 (1990).

[16] B. O'Malley Ph.D. thesis, RMIT, Melbourne, 2001.

[17] D. S. Franzblau, Phys. Rev. B **44**, 4925 (1991).

[18] W. van Megen, T. C. Mortensen, S. R. Williams, and J. Müller, Phys. Rev. E **58**, 6073 (1998).

[19] J. L. Harland, S. I. Henderson, S. M. Underwood, and W. van Megen, Phys. Rev. Lett. **75**, 3572 (1995).

[20] S. I. Henderson, T. C. Mortensen, S. M. Underwood, and W. van Megen, Physica A **233**, 102 (1996).

[21] W. G. T. Kranendonk and D. Frenkel, Mol. Phys. **72**, 679 (1991).

[22] G. A. Mansoori, N. F. Carnahan, K. E. Starling, and T. W. Leland, J. Chem. Phys. **54**, 1523 (1971).

[23] M. J. Murray and J. V. Sanders, Philos. Mag. **42**, 721 (1980).

[24] I. Snook, W. van Megen, and P. N. Pusey, Phys. Rev. A **43**, 6900 (1991).

[25] J. Frenkel, *Kinetic Theory of Liquids* (Oxford University, Oxford, 1946).

[26] M. L. Boas, *Mathematical Methods in the Physical Sciences* (Wiley, New York, 1983).